

arXiv:1307.4549v1 [cond-mat.mes-hall] 17 Jul 2013

e-mail: pierre.lombardo@univ-amu.fr

Hund and pair-hopping signature in transport properties of degenerate nanoscale devices

J. Azema, A.-M. Daré, P. Lombardo

Aix-Marseille Université CNRS, IM2NP UMR 7334, 13397 Marseille, France
e-mail: pierre.lombardo@univ-amu.fr

June 3, 2022

Abstract. We investigate the signature of a complete Coulomb interaction in transport properties of double-orbital nanoscale devices. We analyze the specific effects of Hund exchange and pair hopping terms, calculating in particular stability diagrams. It turns out that a crude model, with partial Coulomb interaction, may lead to a misinterpretation of experiments. In addition, it is shown that spectral weight transfers induced by gate and bias voltages strongly influence charge current. The low temperature regime is also investigated, displaying inelastic cotunneling associated with the exchange term, as well as Kondo conductance enhancement.

PACS. XX.XX.XX No PACS code given

1 Introduction

The strong repulsive Coulomb interaction is responsible for most of the nanoscale device properties like Coulomb blockade, or Kondo effect at low temperature [1, 2, 3]. Local impurity Anderson models [4, 5] are then good candidates to investigate transport properties of these highly confined and strongly correlated systems. Details of local spectroscopic properties are important, particularly since transport channels may consist of sophisticated structures [6]. Consideration of this complexity is essential for a proper interpretation of the transport properties. It allows for example a manipulation of the transition-metal-complex spin states [7]. Also in single-wall carbon nanotube quantum dots, this complexity is responsible for Hund's coupling which directly affects the excitation spectroscopy measurements [8]. Local impurity Anderson model has therefore to be generalized [9, 10, 11, 12] to multi-orbital systems.

However, in this context of orbitally degenerate Anderson model for magnetic impurities or quantum dots, different explicit choices for the Hamiltonian have led to different predictions for the Kondo temperature as a function the Hund's coupling [13]. Besides, in the context of electronic properties of compounds with transition metal ions, thorough discussions about the choice of the local Hamiltonian describing the correlated ions have been published [14, 15, 16]. Even in the simplest case $n = 2$ of the n -orbitally degenerate model, the general Coulomb interaction contains many terms [17]: in addition to intra U and inter orbital U' repulsions, it displays Hund's exchange term J as well as a *pair hopping* parameter J' [18]. This last term is far from being prevalent in literature: to

simplify the calculations, $U' = U$ and $J' = 0$ are often assumed, with few exceptions as in Ref. [19, 20]. Nevertheless, a recent theoretical work concerning lattice multi-orbital Mott systems [21] has shown that both J and J' should be considered to get the correct spectral weight transfer (SWT) upon doping between the various structures composing the electronic density of states. Moreover, the different parameters are not independent, for example, real orbitals lead to $J = J'$. In the case of d -type orbitals one has $U' = U - 2J$. The local Coulomb Hamiltonian is invariant under arbitrary rotation in the spin space, however it is not the case for rotation in the orbital space. To enforce partially this invariance, which is legitimate for degenerate orbitals, one can choose $U' = U - J - J'$ [15]. For $J' = 0$ this leads to $U' = U - J$, and provides invariance under arbitrary rotation in orbital space.

In this paper, we emphasize the importance of taking into account the whole Coulomb Hamiltonian for out of equilibrium properties across a nanoscale device in the Coulomb blockade regime. Specifically, we show that the Coulomb terms J and J' have a major impact on spectral density high energy structures which are involved in the finite bias transport properties. SWT between these structures occurs not only upon varying the gate voltage, but also by changing the bias voltage. This transfer affects deeply the appearance of stability diagrams. At low temperature, inelastic cotunneling processes with a characteristic threshold are driven by the exchange term J .

We therefore provide characteristic signatures which can be experimentally relevant for interpreting stability diagrams and excitation spectroscopy measurements. To this purpose, we calculate local spectral density for a finite applied bias voltage V_{sd} through a doubly-degenerate

quantum dot. The calculation is performed in a fully non-linear manner within the framework of the Keldysh Green's function formalism. More precisely, we use an out-of-equilibrium generalization of the non-crossing approximation (NCA) [22,23], which enables the computation of transport properties in presence of finite voltage across the quantum dot.

2 Model and method

The system under study consists of a doubly degenerate dot coupled to two uncorrelated source and drain contacts. The corresponding Anderson [4] model reads:

$$H = H_d + H_r + H_c,$$

where H_d is the two-orbital ($m = a, b$) local Hamiltonian:

$$H_d = \varepsilon_0 \sum_{m,\sigma} c_{m\sigma}^\dagger c_{m\sigma} + U \sum_m n_{m\uparrow} n_{m\downarrow} - 2J \hat{\mathbf{S}}_a \hat{\mathbf{S}}_b \\ + (U' - \frac{J}{2}) \sum_{\sigma,\sigma'} n_{a\sigma} n_{b\sigma'} + J' \sum_{m \neq m'} c_{m\uparrow}^\dagger c_{m\downarrow}^\dagger c_{m'\downarrow} c_{m'\uparrow}$$

ε_0 is the energy of the degenerate level tuned by the gate voltage $V_g = \varepsilon_0$, the operator $\hat{\mathbf{S}}_m = (\hat{S}_m^x, \hat{S}_m^y, \hat{S}_m^z)$ is the 1/2-spin operator for orbital m . The parameter U denotes the repulsion between electrons occupying the same orbital, $U' = U - J - J'$ is the repulsion between electrons occupying different orbitals, J is the Hund exchange term, and J' is the double hopping term [24]. This last term is systematically present when exchange interactions take place. In the following, calculations are made for two cases: ($J' = J, U' = U - 2J$) and ($J' = 0, U' = U - J$), with $J = U/10$. Note that the Hamiltonian H_d is also relevant for double-quantum dots, however there is no more reason to enforce invariance under rotation in the orbital space in this case, and $U' = U - J - J'$ is no longer required.

The second term H_r describes the left (L) and right (R) leads in standard notations:

$$H_r = \sum_{\substack{\alpha \in \{L,R\} \\ m \in \{a,b\}, k, \sigma}} \varepsilon_{\alpha k} a_{\alpha k m \sigma}^\dagger a_{\alpha k m \sigma}.$$

Finally, H_c accounts for the hybridization tunneling between dot and leads which – we assume – conserves orbital and spin quantum numbers [25]:

$$H_c = \sum_{\substack{\alpha \in \{L,R\} \\ m \in \{a,b\}, k, \sigma}} \left(t_\alpha c_{m\sigma}^\dagger a_{\alpha k m \sigma} + t_\alpha^* a_{\alpha k m \sigma}^\dagger c_{m\sigma} \right).$$

In our calculations, the total electrode density of states $N_\alpha(\varepsilon) = N_{\alpha\uparrow}(\varepsilon) + N_{\alpha\downarrow}(\varepsilon)$ are Gaussian (half-width D) but the results depend very slightly of their particular shape, provided that their width is large compared to the other energy scales of the system. The total hybridization amplitude $\Gamma = \Gamma_L(\bar{\mu}) + \Gamma_R(\bar{\mu})$ will be used as energy unit, where $\Gamma_\alpha(\varepsilon) = \pi t_\alpha^2 N_\alpha(\varepsilon)$ and $\bar{\mu} = \frac{1}{2}(\mu_L + \mu_R)$ is the average chemical potential.

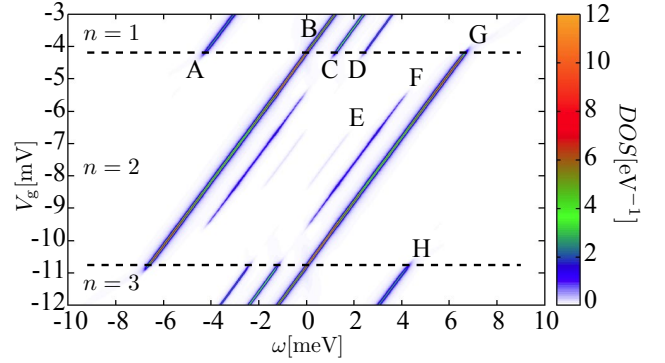


Fig. 1. Local spectral densities for $V_{sd} = 0$ and for different values of V_g from -3 mV to -12 mV. The parameters are $U = 6$ meV, $J = J' = 0.6$ meV, $\Gamma = 0.015$ meV and $k_B T = 0.06$ meV. Energy ω is defined with respect to the shared value of the lead chemical potentials.

In the out of equilibrium regime, a finite voltage bias $V_{sd} = (\mu_L - \mu_R)/e$ is applied symmetrically across the device and the corresponding nonlinear electrical current is given by

$$I_d = \frac{2e}{h} \int [f_L(\varepsilon) - f_R(\varepsilon)] \tau(\varepsilon) d\varepsilon,$$

where h denotes Planck's constant and $-e$ the electronic charge. $f_\alpha(\varepsilon) \equiv f(\varepsilon - \mu_\alpha)$ are the lead Fermi functions, and $\tau(\varepsilon) = \frac{\pi}{4} A(\varepsilon) \Gamma(\varepsilon)$, with $A(\varepsilon) = -\frac{1}{\pi} \text{Im}[\sum_{m,\sigma} G_{m\sigma}(\varepsilon + i\delta)]$, the total dot spectral density. The retarded Green's function $G_{m\sigma}(\varepsilon + i\delta) = \langle\langle c_{m\sigma}; c_{m\sigma}^\dagger \rangle\rangle$ is obtained from a generalized Keldysh-based out-of-equilibrium NCA [22,23]. In the Coulomb blockade regime, the reliability of this approximation is guaranteed since the NCA is known to give accurate results for the spectral density down to temperatures of the order of a fraction of the Kondo temperature T_K [27].

3 Results

3.1 Spectral densities at equilibrium

To investigate the importance of both exchange coupling J and pair hopping J' , we first examine the equilibrium ($V_{sd} = 0$) behavior, by calculating the dot spectral density for various gate voltage V_g . Results are shown in Fig. 1. Varying V_g from -3 mV to -12 mV, the system shifts from quarter-filled ($n = 1$) to three-quarter-filled ($n = 3$). A remarkable property is the structure of the upper Hubbard band for $n = 1$: similarly to the model described in detail by Lee and Phillips [21], we find for the quantum dot under study a characteristic splitting of the upper Hubbard band leading to three peaks whose spectral weights decrease in the proportions of 1.5/1/0.5 (respectively B, C and D in the figure). The dot remains quarter-filled as long as V_g is higher than -4.2 mV. The Coulomb blockade insulating gap is constant and equal to $U - 2J - J'$; B and

C (C and D) are separated by $2J$ ($2J'$). The peak positions and weights of the whole figure can be understood by writing down the eigenstates of the local Hamiltonian H_d . Transition energies between these states are reported in Table 1 and correspond directly to the peak locations, while their amplitudes are related to the degeneracy. Beyond quarter-filling, peak weights are also affected by double and triple occupancy.

$n_1 \rightarrow n_2$	Transition	Energy $-\varepsilon_0$
A: $0 \rightarrow 1$	$ 0,0\rangle \rightarrow 1\rangle$	0
B: $1 \rightarrow 2$	$ 1\rangle \rightarrow \sigma, \sigma\rangle$	$U - 2J - J'$
$1 \rightarrow 2$	$ 1\rangle \rightarrow (\uparrow, \downarrow\rangle + \downarrow, \uparrow\rangle)/\sqrt{2}$	$U - 2J - J'$
C: $1 \rightarrow 2$	$ 1\rangle \rightarrow (\uparrow, \downarrow\rangle - \downarrow, \uparrow\rangle)/\sqrt{2}$	$U - J'$
$1 \rightarrow 2$	$ 1\rangle \rightarrow (\uparrow\downarrow, 0\rangle - 0, \uparrow\downarrow\rangle)/\sqrt{2}$	$U - J'$
D: $1 \rightarrow 2$	$ 1\rangle \rightarrow (\uparrow\downarrow, 0\rangle + 0, \uparrow\downarrow\rangle)/\sqrt{2}$	$U + J'$
E: $2 \rightarrow 3$	$(\uparrow\downarrow, 0\rangle + 0, \uparrow\downarrow\rangle)/\sqrt{2} \rightarrow 3\rangle$	$2U - 3J - 3J'$
F: $2 \rightarrow 3$	$(\uparrow\downarrow, 0\rangle - 0, \uparrow\downarrow\rangle)/\sqrt{2} \rightarrow 3\rangle$	$2U - 3J - J'$
$2 \rightarrow 3$	$(\uparrow, \downarrow\rangle - \downarrow, \uparrow\rangle)/\sqrt{2} \rightarrow 3\rangle$	$2U - 3J - J'$
G: $2 \rightarrow 3$	$(\uparrow, \downarrow\rangle + \downarrow, \uparrow\rangle)/\sqrt{2} \rightarrow 3\rangle$	$2U - J - J'$
$2 \rightarrow 3$	$ \sigma, \sigma\rangle \rightarrow 3\rangle$	$2U - J - J'$
H: $3 \rightarrow 4$	$ 3\rangle \rightarrow \uparrow\downarrow, \uparrow\downarrow\rangle$	$3U - 3J - 2J'$

Table 1. Transition energies between local eigenstates of H_d for two orbitals. Hund's coupling and pair hopping partially remove the degeneracy of doubly occupied states. $|1\rangle$ represents any state with one electron and $|3\rangle$ represents any 3-electron state. Letters from A to H refer to Fig. 1.

Upon decreasing V_g , we observe, together with a sharp increase of n , a significant transfer of spectral weight between the different bands. SWT is a general property of correlated systems [28,29], in contrast to the rigid band patterns of uncorrelated ones, and occurs even for the one orbital case. In case of orbital degeneracy, SWT is more sophisticated because of additional orbital degrees of freedom. As shown in Fig. 1, J and J' strongly affect the transfer which arises sequentially when transitions involving two-electron states (B, C, D) cross the Fermi level: the first crossing (B) triggers the simultaneous disappearance of bands A, C and D. The corresponding spectral weight is redistributed between B and G, causing a sudden increase of B amplitude. Further increasing V_g , B amplitude is reduced by the resurgence of C and D. This non-monotonic SWT has no equivalent in the absence of J and J' . This behavior obtained for $V_{sd} = 0$ will undoubtedly have major implications on the transport properties in the finite bias regime. Moreover, a finite V_{sd} will lead to additional SWT. This will be highlighted in the following results for spectral densities, excitation spectrum and stability diagrams.

3.2 Nonlinear transport and excitation spectrum

Let us turn to finite bias regime, first calculating the excitation spectrum dI_d/dV_g . This quantity is experimentally accessible [8] and allows direct visualization of the different transport channels. To reveal the influence of J and J' ,

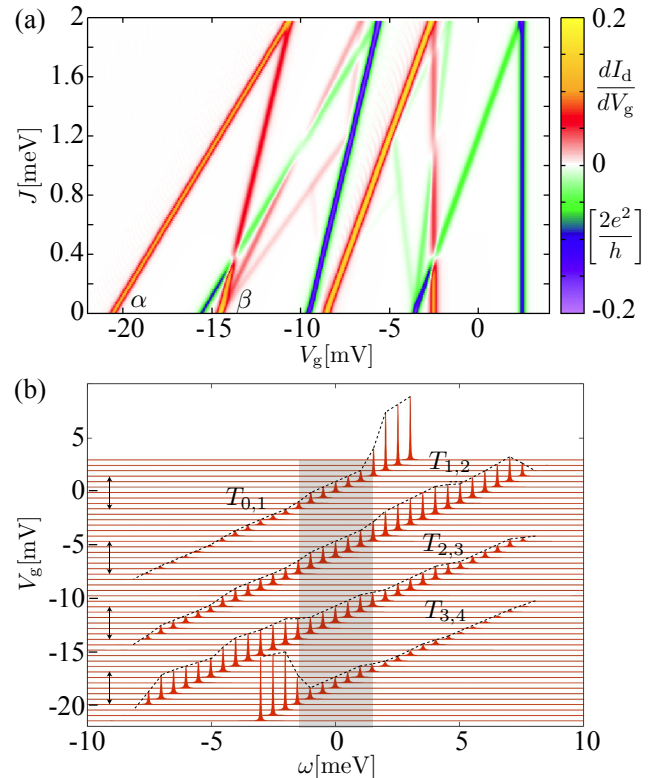


Fig. 2. (a) Excitation spectrum diagrams dI_d/dV_g with respect to $J = J'$ and V_g . Other parameters are $U = 6$ meV, $\Gamma = 0.015$ meV, $V_{sd} = 5$ mV and $k_B T = 0.06$ meV. (b) Spectral densities for V_g going from 3 mV to -21 mV, $J = J' = 0$ and $V_{sd} = 3$ mV. Energy ω is defined with respect to the average of μ_L and μ_R . $T_{m,n}$ corresponds to the transition between two local states containing respectively m and n electrons. The conducting regime (indicated by double arrows) is achieved when a peak lies inside the bias window.

we plot the excitation spectrum as a function of V_g and J . Results obtained for $V_{sd} = 5$ mV are displayed in Fig. 2(a). The various drifts upon raising J can be understood by looking at the last column of Table 1. Due to the identity $J' = J$, these drifts range from $-6J$ to $+J$, leading to several crossings. For increasing V_g , positive contributions correspond to the entering of a spectral density peak into the bias window $[-V_{sd}/2, V_{sd}/2]$, whereas negative ones correspond to peaks leaving this window. A given peak therefore generates a pair of parallel lines, one positive and the other negative, separated by V_{sd} . For $J = 0$, these pairs are spaced by U . Note that positive contributions display a great diversity of amplitudes, some of them being nearly vanishing. This can be understood by studying spectral densities of Fig. 2(b), where for the sake of clarity, we choose $J = J' = 0$ in order to have fewer peaks, and $V_{sd} = 3$ mV (far from U) to obtain clearly separated *entering in* and *exit from* bias window (light grey in the figure). Upon increasing V_g , the peak $T_{3,4}$ enters the bias window for $V_g = -3U - V_{sd}/2$, and leaves it V_{sd} further. A

similar process is followed by the peaks $T_{2,3}$, $T_{1,2}$ and $T_{0,1}$, but their amplitudes in the bias window are different, resulting in different values of the current through the dot: this accounts for the magnitude difference between points α and β for example, in Fig. 2(a).

Furthermore, Fig. 2(b) clearly shows a significant SWT upon tuning V_g . The spectral density for $V_g = 3$ mV corresponds to a number of electron equal to zero. Thus, the weight is concentrated in a single peak corresponding to the transition between the empty state and the singly occupied state $T_{0,1}$. Unlike the equilibrium case in which SWT occurs when a structure crosses the Fermi level [29], a finite bias two-stage SWT happens when a peak crosses one of the two chemical potentials μ_L or μ_R . Apart from these coincidences, the spectral weights remain constant. This leads to a dot occupation presenting the appearance of a series of plateaus, whose values are not only the integers of the equilibrium case.

3.3 Stability diagrams

Stability diagrams are obtained by representing the differential conductance dI_d/dV_{sd} as a function of V_g and V_{sd} . They are shown in Fig. 3. In the Coulomb blockade regime, stability diagrams exhibit well-known diamond-shaped structures. For $J = J' = 0$, in Fig. 3(a), the stability diagrams are composed of eight lines forming Coulomb diamonds whose diagonal lengths are $2U$ and U . The central diamond corresponds to $n = 2$ and the two that surround it to $n = 3$ (left) and $n = 1$ (right). The average dot occupancies above and below these diamonds are non-integer. Along the diamond lines, the amplitude is highly variable. For example, the amplitude is close to 0.088 in L and to 0.055 in M. This is a consequence of the large weight asymmetry between the upper and lower Hubbard bands for $n = 1$. The inset with spectral density corresponding to I, J and K, enables to understand how SWT drives Coulomb diamond amplitudes at constant V_g : from I to J the structure entering the bias window (in light grey in the inset) increases significantly, leading to an important current jump; while from J to K the corresponding SWT occurs mainly between two structures inside the window, with a weaker influence on the current variation. For $J \neq 0$ and $J' = 0$, Fig. 3(b), the central diamond is wider (corresponding to a gap $U + J$) and the side diamonds simultaneously shrink (gap $U - 2J$). For $J' = J \neq 0$, Fig. 3(c), new structures appear and the narrowing of side diamonds is more pronounced ($U - 3J$). The hierarchy of amplitude between the different lines is directly related to the energy differences between doubly occupied states (see Fig. 1 and Table 1).

The central part of stability diagram at lower temperature, revealing the cotunneling regime, is displayed in Fig. 4 for $J \neq 0$ and $J' = 0$. The parameters, different from those of Fig. 3(b), have been selected to enhance the visibility of this phenomenon. In the central diamond ($n = 2$), we observe a clear occurrence of inelastic cotunneling processes displaying a characteristic threshold [30]. This threshold is given by the energy difference

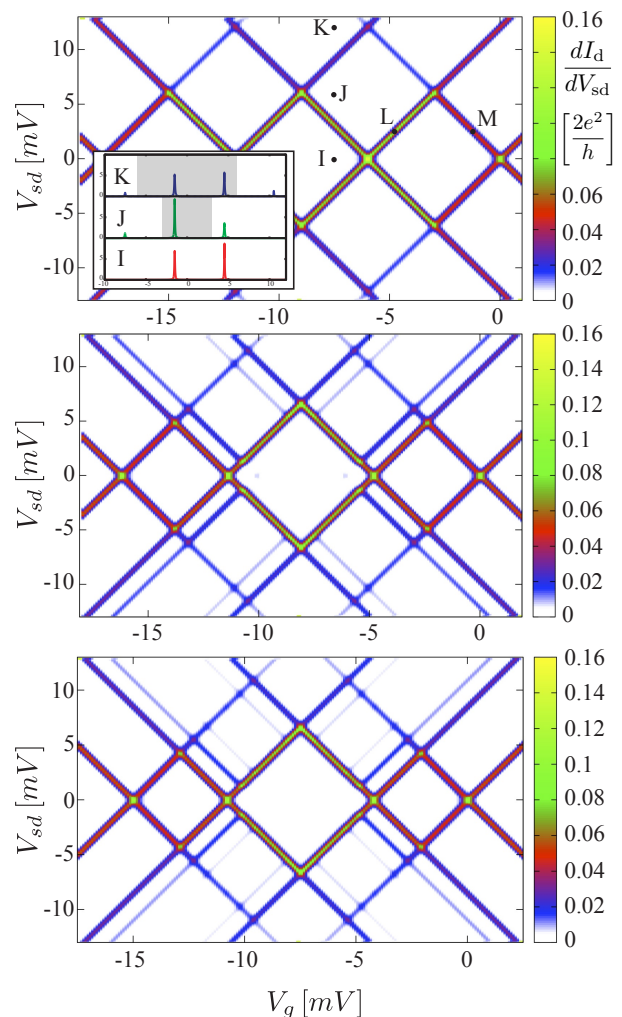


Fig. 3. Stability diagrams (a) for $J = J' = 0$, (b) for $J = 0.6$ meV and $J' = 0$, (c) for $J = J' = 0.6$ meV. Other parameters are $U = 6$ meV, $\Gamma = 0.015$ meV and $k_B T = 0.06$ meV. The inset in (a) displays spectral density corresponding to I, J, K.

between two-particle states, namely $2J$. A similar behavior has been observed using a master equation approach in a double-quantum dot in which the cotunneling threshold is the exchange energy [31]. A careful examination of the figure shows a zero-biased conductance enhancement which is due to the Kondo effect. The Kondo temperature is lower for a spin $S = 1$ than for $S = 1/2$ [32] and therefore the enhancement is more pronounced in side diamonds where $n = 1$ and $n = 3$ respectively.

4 Conclusion

To summarize, we have shown that Hund's rule exchange coupling and pair hopping strongly affect transport properties in the Coulomb blockade regime. If the multi-orbital

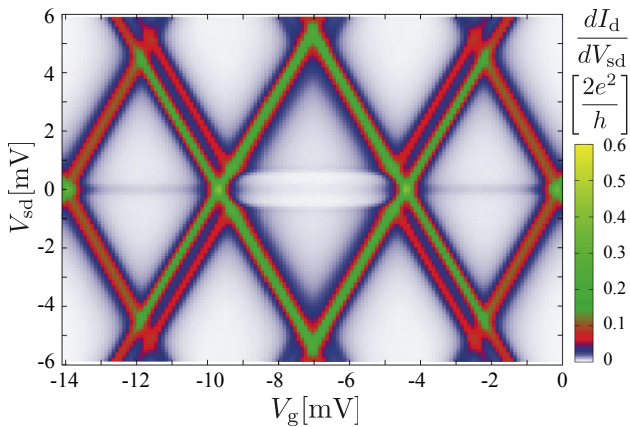


Fig. 4. Low temperature stability diagram for $J = 0.3$ meV, $J' = 0$, $U = 5$ meV, $\Gamma = 0.05$ meV, and $k_B T = 0.01$ meV.

Anderson model in the atomic limit can provide the Coulomb diamond positions, their amplitudes however result from spectral weight transfers. Those can only be determined by a proper treatment of correlations in the out of equilibrium regime, especially since the bias voltage variation itself causes transfer. The comparative study of the results obtained with the full Hamiltonian on the one hand, and the Hamiltonian containing only the Hund's coupling on the other hand, clearly indicates the importance of the pair-hopping term, yet rarely considered. In particular, the analysis of experimental stability diagrams without considering pair-hopping narrowing of side diamonds, leads to overestimate the exchange term.

References

1. R. Hanson, L. P. Kouwenhoven, J. R. Petta, S. Tarucha, and L. M. K. Vandersypen, *Rev. Mod. Phys.* **79**, 1217 (2007)
2. J. Nygard, D. H. Cobden, P. E. Lindelof, *Nature* **408**, 342 (2000)
3. J. Park, *et al.* *Nature* **417**, 722 (2002)
4. P. W. Anderson, *Phys. Rev.* **124**, 41 (1961)
5. Y. Meir, N. S. Wingreen, and P. A. Lee, *Phys. Rev. Lett.* **70**, 2601 (1993)
6. S. Tarucha, D. G. Austing, T. Honda, R. J. van der Hage, and L. P. Kouwenhoven, *Phys. Rev. Lett.* **77**, 3613 (1996); L. P. Kouwenhoven, T. H. Oosterkamp, M. W. S. Danoesastro, M. Eto, D. G. Austing, T. Honda, and S. Tarucha, *Science* **278**, 1788 (1997); L. P. Kouwenhoven, D. G. Austing, and S. Tarucha, *Rep. Prog. Phys.* **64**, 701 (2001)
7. E.A. Osorio, K. Moth-Poulsen, H.S.J van der Zant, J. Paaske, P. Hedegård, K. Flensberg, J. Bendix, T. Bjørnholm, *Nano Letters* **10**, 105 (2010)
8. S. Moriyama, T. Fuse, M. Suzuki, Y. Aoyagi, and K. Ishibashi, *Phys. Rev. Lett.* **94**, 186806 (2005)
9. T. Kita, R. Sakano, T. Ohashi, and S. Suga, *J. Phys. Soc. Jpn.* **77**, 094707 (2008)
10. D. E. Logan, C. J. Wright, and M. R. Galpin, *Phys. Rev. B* **80**, 125117 (2009)
11. S. Florens, A. Freyn, N. Roch, W. Wernsdorfer, F. Balestro, P. Roura-Bas, and A. A. Aligia, *J. Phys.: Condens. Matter* **23**, 243202 (2011)
12. R. Sakano, Y. Nishikawa, A. Oguri, A. C. Hewson, and S. Tarucha, *Phys. Rev. Lett.* **108**, 266401 (2012)
13. Y. Nishikawa, and A.C. Hewson, *Phys. Rev. B* **86**, 245131 (2012)
14. J. Kanamori, *J. Phys. Chem. Solids* **10**, 87 (1959)
15. E. Dagotto, T. Hotta, and A. Moreo, *Phys. Rep.* **344**, 1 (2001)
16. A. M. Oleś, G. Khaliullin, P. Horsch, and L.F. Feiner, *Phys. Rev. B* **72**, 214431 (2005)
17. The general Coulomb Hamiltonian can be expressed as follows: $H_C = 1/2 \sum_{i,j,k,l} V_{ijkl} c_{i\sigma}^\dagger c_{j\sigma'}^\dagger c_{l\sigma'} c_{k\sigma}$. The intra- and inter-orbital interactions are respectively $U = V_{iiii}$ and $U' = V_{ijij}$, while the Hund and pair-hopping parameters are $J = V_{ijji}$ and $J' = V_{ijjj}$.
18. An exchange interaction can also arise in the context of double quantum dots due to hybridization between orbitals. This kinetic exchange favors antiferromagnetic spin arrangement while Hund exchange is ferromagnetic. Besides, J' should not be confused with the pair tunneling process discussed by M. Leijnse, M. R. Wegewijs, and M. H. Hettler, *Phys. Rev. Lett.* **103**, 156803 (2009); these processes are included in our treatment.
19. X. Wang and A. J. Millis, *Phys. Rev. B* **81**, 045106 (2010)
20. S. Yang, X. Wang, and S. Das Sarma, *Phys. Rev. B* **83**, 161301(R) (2011)
21. W.-C. Lee and P. W. Phillips, *Phys. Rev. B* **84**, 115101 (2011)
22. N. S. Wingreen and Y. Meir, *Phys. Rev. B* **49**, 11040 (1994)
23. M. H. Hettler, J. Kroha, and S. Hershfield, *Phys. Rev. B* **58**, 5649 (1998)
24. The Coulomb Hamiltonian also contains an occupation modulated hopping [20] that we do not consider here.
25. In some systems, conservation of orbital quantum number is expected on symmetry grounds as in vertical quantum dots. Furthermore, it can lead to orbital Kondo effect, for example in carbon nanotube quantum dot. However it is not always realized, see for example [26] and references therein.
26. J. S. Lim, M.-S. Choi, M. Y. Choi, R. López, and R. Aguado, *Phys. Rev. B* **74**, 205119 (2006)
27. P. Roura-Bas, *Phys. Rev. B* **81**, 155327 (2010); L. Tosi, P. Roura-Bas, A. M. Llois, and A.A. Aligia, *Physica B* **407**, 3263 (2012).
28. M. B. J. Meinders, H. Eskes, and G. A. Sawatzky, *Phys. Rev. B* **48**, 3916 (1993)
29. P. Lombardo and G. Albinet, *Phys. Rev. B* **65**, 115110 (2002)
30. S. De Franceschi, S. Sasaki, J. M. Elzerman, W. G. van der Wiel, S. Tarucha, and L. P. Kouwenhoven, *Phys. Rev. Lett.* **86**, 878 (2001)
31. V. N. Golovach and D. Loss, *Phys. Rev. B* **69**, 245327 (2004)
32. S. Sasaki, S. De Franceschi, J. M. Elzerman, W. G. van der Wiel, M. Eto, S. Tarucha, and L. P. Kouwenhoven, *Nature* **405**, 764 (2000), and references therein.